# Kinematic Analysis of a Novel 3-DOF Parallel Robot with 4 Limbs

WANG ZHONGFEI, QIAN XIANFA, JI SHIMING, WAN YUEHUA, PAN YAN
The MOE Key Laboratory of Mechanical Manufacture and Automation
Zhejiang University of Technology
Hangzhou, Zhejiang
CHINA

*Abstract:* A novel 3-DOF spatial parallel robot with four identical $PRP_AR$ kinematic limbs is proposed, which belongs to redundant actuated parallel robot, and its kinematics including motion property, inverse problem, forward problem and workspace are studied. After a short description of the novel architecture, then its kinematic modeling is built through the D-H parametric notions and the coordinate transformation technique, which verifies that this novel parallel robot has pure spatial translational motion. Follow these analysis, the inverse and forward kinematic problems are solved with analytical closed-form, its inverse problem has only one solution for each actuated joints, and its forward problem has only one preferred solution to certain assembly manner. Finally, a case study is analyzed by numerical method, including the determination of workspace, simulation of the inverse and forward kinematic solutions.

*Key-Words:* Redundant Actuated Parallel Robot D-H notations Kinematics Workspace

## 1 Introduction

The parallel robots (PRs) offer obvious advantages over serial ones, such as high structural stiffness, position accuracy and good dynamic performance. However, the PRs have smaller and irregular shape workspace, lower dexterity. Most of the PRs proposed in the literature have a non-redundant structure. To overcome some of the foregoing disadvantages, redundant actuated parallel robots (RAPRs) have been designed [1]. The RAPRs refers to the use of more actuators than are strictly necessary to control the robot, but without increasing the mobility. In general, actuators redundancy can be obtained either by replacing passive joints of an existing PR with active ones or by introducing additional limbs in an existing system. Some researchers have investigated this subject in PRs. Most of their studies have focused on planar RAPRs [2-5], but a few spatial ones [6-10].

The 3-DOF redundant actuated spatial translational parallel robots (RASTPRs) have been found in [8-10]. Joshi and Tsai [10] performed a detailed comparison between a 3-UPU and the so-called Tricept Robot [8,9] regarding the kinematic, workspace and stiffness properties of the mechanisms. Complete kinematic modeling and Jacobian analysis of such robots have not received much attention so far and are still regarded as an interesting problem in parallel robotics research.

In this paper, a novel RASTPR is proposed, which has a symmetrical architecture with four identical $PRP_AR$ topological limbs, so any a limb acts as redundant one when controlling. The novel RASTPR allows finding analytical closed-form solutions for both inverse and forward kinematic problems. It is of great importance notice that the forward kinematics solution is a key element in closed loop position control of PRs. Additionally, it has regular shape workspace, which is an advantage compared with the other PRs in the literatures.

## 2 Description of the Novel RASTPR

The CAD model of the novel RAPRs is shown in Fig. 1. It is comprised of the base and the moving platform with a gripper by means of four identical limbs, which has $PRP_AR$ topology, from the base to moving platform along the limb. The moving platform is a square. In literature such architecture is conventionally called 4-$PRP_AR$ to indicate the sequence of the joints in the limbs. For brevity, P and R respectively indicate prismatic and revolute pairs, and $P_A$ stands for a combined joint of a planar 4-bar parallelogram loop. Its prototype is shown in Fig. 2.

From Fig. 1, we can see that each limb of the novel RAPR possesses one prismatic pair (P) as actuated joint which is connected to the base, two revolute pairs (R) and one combined joint of a planar 4-bar parallelogram loop ($P_A$). On the whole, the four actuated P joints are parallel mutually, their axes are normal to the base, and the four connected points of P joints on the base are vertex of a square. The shape of the moving platform is a square. For one of limbs,

a $P_A$ joint posited in between the first R joint which is adjacent P joints and the last R joint which is adjacent the moving platform, the two R joints axes are parallel, and these axes and the R pairs axes of vertexes of $P_A$ joint are perpendicular.

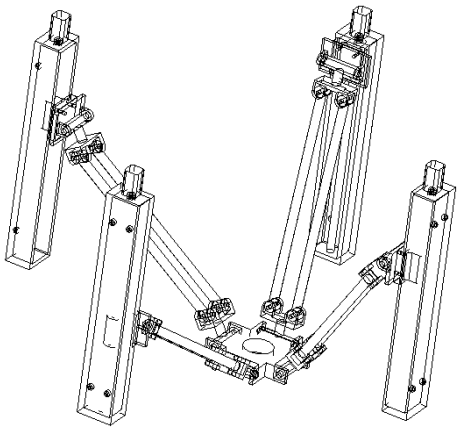

Fig. 1. The CAD model of the RASTPR

Fig. 2. A protype of the RASTPR

# 3 The kinematic modeling

## 3.1 The joints coordinate systems and the D-H parameters

As a matter of convenience, to describle the geometrical parameters of the links and joints in a limb starting from the base for any limb, we number the links sequentially from 0 to $n$, and joints from 1 to $n$, here $n$=7. Following Denavit & Hartenberg (D-H) convention and rules, a Cartesian coordinate system is attached to each link. Firstly, we assign a global coordinate system on the base, $O$-$XYZ$, as

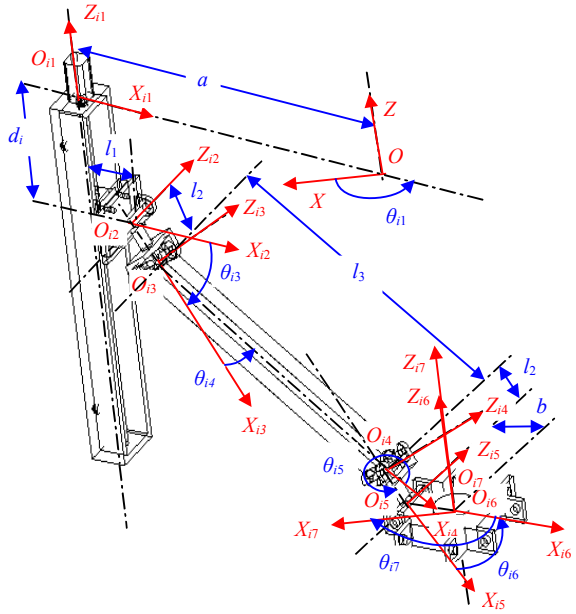


Fig. 3. The coordinate systems and the parameters of the links and joints of the $i$-th limb

coordinate system $O_{i0}$ of each limb, point $O$ is coincided to central of the base, the direction of $X$ axis is towards $O_{11}$, and the $Z$ axis is normal to the base. Additionally, we sign that the character $i$ denotes the number of the limbs, i.e. $i$=1,2,3,4. Analysising the $i$-th limb, we arrange the coordinate systems as shown in Fig.3 ($i$=1, 2, 3, 4).

Table 1. The geometrical parameters of the four limbs

| *No.* | $a_{ij}$ | $\beta_{ij}$ | $d_{ij}$ | $\theta_{ij}$ |
|---|---|---|---|---|
| 1 | -$a$ | 0 | 0 | $\theta_{i1}$ |
| 2 | $l_1$ | 3$\pi$/2 | $d_i$ | 0 |
| 3 | $l_2$ | $\pi$/2 | 0 | $\theta_{i3}$ |
| 4 | $l_3$ | 0 | 0 | $\theta_{i4}$ |
| 5 | $l_2$ | 3$\pi$/2 | 0 | $\theta_{i5}$=2$\pi$-$\theta_{i4}$ |
| 6 | $b$ | $\pi$/2 | 0 | $\theta_{i6}$=2$\pi$-$\theta_{i3}$ |
| 7 | 0 | 0 | 0 | $\theta_{i7}$=2$\pi$-$\theta_{i1}$ |

*Note: $\theta_{i1}$ = (3-i)$\pi$/2, i=1, 2, 3, 4. Where, all the parameters are shown in Fig. 3.*

Based on D-H parametric notation for the coordinate systems, the links and joints parameters on the four limbs can be tabulated from Table 1, in which $a_{ij}$ denotes the parallel translation of origins along $x_{ij}$ and $d_{ij}$ denotes the parallel translation along $z_{ij-1}$. The parameter of $\beta_{ij}$ denotes the rotations from $z_{ij-1}$ to $z_{ij}$, around $x_{ij}$, and $\theta_{ij}$ denotes the ratations from $x_{ij-1}$ to $x_{ij}$, around $z_{ij-1}$. Here, $i$= 1,2,3,4, denotes the number of limbs, and $j$=1, ... ,7, denotes the number of joints on a limb.

## 3.2 The kinematic modeling

The general matrix form of the transformation

relationships between the local coordinate systems of two adjacent links can be derived as follows,

$$ {}^{i}T_{i+1} = \begin{bmatrix} c\theta & -s\theta & 0 & d_x c\theta \\ c\alpha \cdot s\theta & c\alpha \cdot c\theta & -s\alpha & d_x c\theta \cdot s\theta - d_z c\alpha \\ s\alpha \cdot s\theta & s\alpha \cdot c\theta & c\alpha & d_x s\theta \cdot s\theta + d_z c\alpha \\ 0 & 0 & 0 & 1 \end{bmatrix} \quad (1) $$

where, $s\alpha$, $s\theta$, $c\alpha$, and $c\theta$, are $sin(\alpha)$, $sin(\theta)$, $cos(\alpha)$, and $cos(\theta)$, respectively.

By the parameters in Table 1 and the relationship of the coordinate transformation (1), for the first limb, i.e. $i$=1, the D-H transformation matrices of the all links are obtained. Then, the position matrix of gripper on the moving platform with respect to the global coordinate system is obtained in terms of the first limb:

$$ {}^{O}A_{17} = \begin{bmatrix} 1 & 0 & 0 & e - 2l_2 c\theta_{13} - l_3 c\theta_{13} \cdot c\theta_{14} \\ 0 & 1 & 0 & -l_3 s\theta_{14} \\ 0 & 0 & 1 & -2l_2 s\theta_{13} - l_3 s\theta_{13} \cdot c\theta_{14} + d_1 \\ 0 & 0 & 0 & 1 \end{bmatrix} \quad (2) $$

where $s\theta_{i,j}$ and $c\theta_{i,j}$ denote $sin(\theta_{i,j})$ and $cos(\theta_{i,j})$ respectively, $e = a\text{-}b\text{-}l_1$.

Similarly, for other three limbs, the position matrices of the gripper on the moving platform are obtained.

$$ {}^{O}A_{27} = \begin{bmatrix} 1 & 0 & 0 & l_3 s\theta_{24} \\ 0 & 1 & 0 & e - 2l_2 c\theta_{23} - l_3 c\theta_{23} c\theta_{24} \\ 0 & 0 & 1 & -2l_2 s\theta_{23} - l_3 s\theta_{23} c\theta_{24} + d_2 \\ 0 & 0 & 0 & 1 \end{bmatrix} \quad (3) $$

$$ {}^{O}A_{37} = \begin{bmatrix} 1 & 0 & 0 & -e + 2l_2 s\theta_{33} + l_3 c\theta_{33} c\theta_{34} \\ 0 & 1 & 0 & l_3 s\theta_{34} \\ 0 & 0 & 1 & -2l_2 s\theta_{33} - l_3 s\theta_{33} c\theta_{34} + d_3 \\ 0 & 0 & 0 & 1 \end{bmatrix} \quad (4) $$

$$ {}^{O}A_{47} = \begin{bmatrix} 1 & 0 & 0 & l_3 s\theta_{44} \\ 0 & 1 & 0 & -e + 2l_2 c\theta_{43} + l_3 c\theta_{43} c\theta_{44} \\ 0 & 0 & 1 & -2l_2 s\theta_{43} - l_3 s\theta_{43} c\theta_{44} + d_4 \\ 0 & 0 & 0 & 1 \end{bmatrix} \quad (5) $$

Based on the closed-chain of parallel robot, the position matrices of the gripper on the moving platform derived from each kinematic limb are equivalent, i.e.

$$ {}^{O}A_{17} = {}^{O}A_{27} = {}^{O}A_{37} = {}^{O}A_{47} \quad (6) $$

is the kinematic modeling of the proposed PR.

Then, by (2)~(6), we discover that the partition of the orientational elements is an identity matrix for any limbs. Obviously, when the moving platform moves, there is only pure spatial translational motion. In other words, the motion property of the proposed PR has 3-DOF pure translational movement, so is called the redundant actuated spatial translational parallel robot.

# 4 Kinematic Analysis

## 4.1 Inverse Kinematics

Suppose that the structural parameters are given, the purpose of the inverse kinematics is to solve the actuated and passive joints variables from a given pose of the gripper on the moving platform. For the inverse kinematics of the proposed RASTPR, the position coordinates ($x$, $y$, $z$) of the gripper are given but the sliding distance $d_i$ of actuated P joints and all rotational joint variables $\theta_{ij}$ are unknown.

By the previous section, for the proposed RASTRPR with pure spatial translational motion, we needn't concern the rotational pose of the moving platform. From the last column element of each position matrix of the gripper on the moving platform, which indicates the position, thus we get three equations. Solving three equations simultaneously, the actuated variables $d_i$ ($i$=1,2,3,4) are obtained with corresponding to the given ($x$, $y$, $z$).

For the first limb, obtain the three equations from the (2) :

$$ \begin{aligned} x &= e - 2l_2 c\theta_{13} - l_3 c\theta_{13} c\theta_{14}, \\ y &= -l_3 s\theta_{14}, \\ z &= -2l_2 s\theta_{13} - l_3 s\theta_{13} c\theta_{14} + d_4 \end{aligned} \quad (7) $$

Where, $-\pi/2 \le \theta_{1j} \le \pi/2$, for $j$=3, 4. The interval of $\theta_{ij}$ for $i$=2, 3, 4 are the same in the following analyses.

Considering the interval of $\theta_{13}$ and $\theta_{14}$, solving (7) yields,

$$ d_1 = z \pm \sqrt{(2l_2 + \sqrt{l_3^2 - y^2})^2 - (x - e)^2} \quad (8) $$

Meanwhile, we get the expressions of $\theta_{13}$ and $\theta_{14}$ from,

$$ \cos\theta_{13} = (e - x)/(2l_2 + \sqrt{l_3^2 - y^2}) \quad (9) $$

$$ \cos\theta_{14} = \sqrt{l_3^2 - y^2}/l_3 \quad (10) $$

Similarly, for the second limb, from the (3), yields,

$$ d_2 = z \pm \sqrt{(2l_2 + \sqrt{l_3^2 - x^2})^2 - (y - e)^2} \quad (11) $$

$$ \cos\theta_{23} = (e - y)/(2l_2 + \sqrt{l_3^2 - x^2}) \quad (12) $$

$$ \cos\theta_{24} = \sqrt{l_3^2 - x^2}/l_3 \quad (13) $$

For the third limb, yields,

$$d_3 = z \pm \sqrt{(2l_2 + \sqrt{l_3^2 - y^2})^2 - (x+e)^2} \quad (14)$$

$$\cos\theta_{33} = (-e + x)/(2l_2 + \sqrt{l_3^2 - y^2}) \quad (15)$$

$$\cos\theta_{24} = \sqrt{l_3^2 - y^2}/l_3 \quad (16)$$

Then, for the forth limb, yields,

$$d_4 = z \pm \sqrt{(2l_2 + \sqrt{l_3^2 - x^2})^2 - (y-e)^2} \quad (17)$$

$$\cos\theta_{43} = (-e + y)/(2l_2 + \sqrt{l_3^2 - x^2}) \quad (18)$$

$$\cos\theta_{44} = \sqrt{l_3^2 - x^2}/l_3 \quad (19)$$

It can be observed that there are two solutions theoretically for each actuated variable, which are mirroring about one plane, hence there are totally sixteen sets of possible solutions for a given position of the moving platform. All possible configurations are shown in Fig.4. In this paper, to enhance the stiffness of the manipulator, the configurations from (*b*) to (*o*) are eliminated. In the two left, the configuration (*a*) is corresponding to case of "+" in (8), (11), (14) and (17), and for (*p*) if "-". Here, by the model shown in Fig. 1, the configuration (*a*) is chosen, thus the proposed RASTPR has only one inverse kinematic solution for each actuated joint.

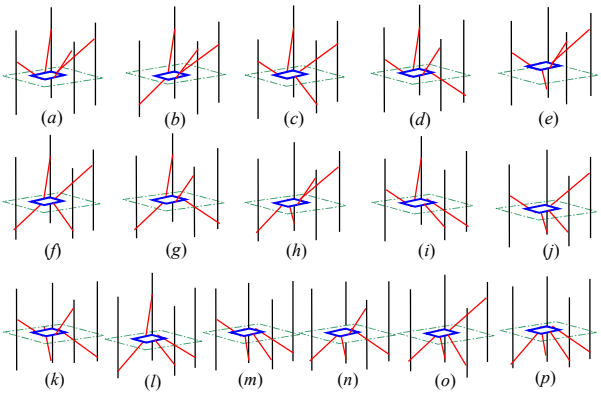


Fig. 4. All possible configurations of the RASTPR

### 4.2 Forward Kinematics

The purpose of forward kinematics is to find the position of the gripper on the moving platform when the actuated joint variables are given.

For the first limb, considering the $-\pi/2 \le \theta_{13} \le \pi/2$ and $-\pi/2 \le \theta_{14} \le \pi/2$, from (7), obtain a second-order algebra equation with respect to unknown *x*, *y*, *z* variables through eliminating of $\theta_{13}$ and $\theta_{14}$.

$$(x-e)^2 + (z-d_1)^2 = (2l_2 + \sqrt{l_3^2 - y^2})^2 \quad (20)$$

Similarly, for the second limb, obtains

$$(y-e)^2 + (z-d_2)^2 = (2l_2 + \sqrt{l_3^2 - x^2})^2 \quad (21)$$

For the third limb, obtains

$$(x+e)^2 + (z-d_3)^2 = (2l_2 + \sqrt{l_3^2 - y^2})^2 \quad (22)$$

For the forth limb, obtains

$$(y+e)^2 + (z-d_4)^2 = (2l_2 + \sqrt{l_3^2 - x^2})^2 \quad (23)$$

Then, the forward kinematic problem is solved by found solutions of a set of equations (20)~(23). Subtracting (22) from (20), and (23) from (21) respectively yields

$$x = k_1 z + k_{01} \quad (24)$$

$$y = k_2 z + k_{02} \quad (25)$$

where $k_{01} = (d_1^2 - d_3^2)/4e$, $k_{02} = (d_2^2 - d_4^2)/4e$, $k_1 = (d_3 - d_1)/2e$, $k_2 = (d_4 - d_2)/2e$.

Substituting (24) and (25) into (20), obtain a fourth-degree polynomial in single unknown *z*.

$$\sum_{i=0}^{4} A_i z^i = 0 \quad (26)$$

where the coefficients $A_i$ depend on the input variables and geometrical parameters of the robot, $A_0 = B_0^2 + 16l_2^2(k_{02}^2 - l_3^2)$, $A_1 = 2(B_0B_1 + 16k_2k_{02}l_2^2)$, $A_2 = 2B_0B_2 + B_1^2 + 16k_2^2l_2^2$, $A_3 = 2B_1B_2$, $A_4 = B_2^2$, $B_0 = (k_{01}^2 + k_{01}^2 + d_1^2 + e^2 - 4l_2^2 - l_3^2 - 2k_{01}e)$, $B_1 = 2(k_1k_{01} + k_2k_{02} - k_1e - d_1)$, and $B_2 = (k_1^2 + k_2^2 + 1)$.

Equation (26) provides at most four solutions for *z* in the complex field. For any of them, a unique value for *x* and *y* may be obtained via (24) and (25) in sequence. Thus, there are total of 4 sets of *x*, *y*, and *z*.

## 5 A case study

In order to illustrate the derived inverse and forward kinematic solutions, a case study is implemented to identify the configurations and workspace of the robot through a numerical method. The geometrical parameters of a RASTPR are $a$=300$mm$, $b$=50$mm$, $l_1$= $l_2$=30$mm$, $l_3$=250$mm$, and the maximal stroke of actuated P joints is 500$mm$, respectively.

### 5.1 Inverse kinematic simulation

Based on the derived analytical closed-form solutions of inverse kinematics in the previous section, we can identify the input values $d_i$ and the unknown variables $\theta_{i3}$, and $\theta_{i4}$, ($i$=l, 2, 3, 4) at the given position *x*, *y*, *z*. Suppose that guiding the gripper on the moving platform along a spatial path,

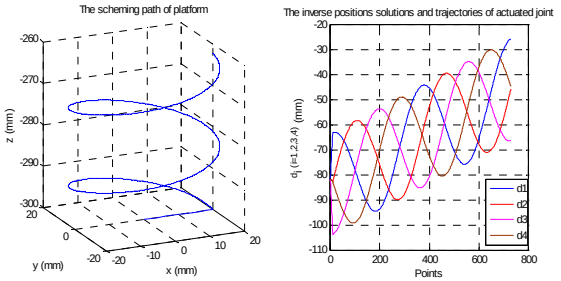


(*a*) (*b*)

Fig. 5. The inverse kinematic simulation

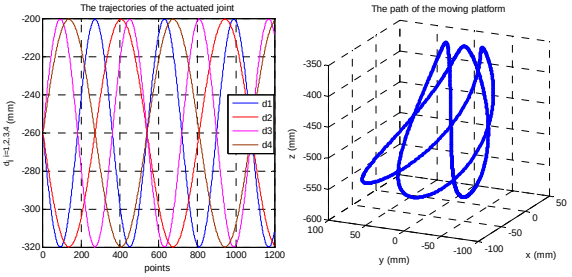


(*a*) (*b*)

Fig. 6. The forward kinematic simulation

which as shown in Fig. 5 (*a*), i.e. a helical path, the starting point of scheming path locates at (0, 0, -300)*mm*, the radius and pitch of helix are 20*mm* and 3*mm* respectively, and the end point is at (20, 0, –262.3532)*mm*. Then, applying the derived analytical solutions in previous section, we can find the corresponding actuated joints trajectories shown in Fig. 5 (*b*).

## 5.2 Forward kinematic simulation

From the forward kinematic solutions in previous section, (26) provides at most four solutions for $z$ in the complex field, $x$ and $y$ may be obtained via (24) and (25), thus we can get four sets of possible solutions for $x$, $y$, and $z$. Although the number of solutions is considerably much, it can be shown that only one solution feasible and the preferred solution can be determined by the assembly manner.

In order to illustrate the derived forward kinematic solutions, taking the mentioned geometrical parameters above, let $d_1 = 0$, $d_2 = 0$, $d_3 = 0$, and $d_4 = 0$. Then, the polynomial (26) becomes

$$z^4 - 35400\, z^2 - 586710000 = 0 \qquad (27)$$

which has four solutions for $z$, where suppose that the values of z have no meaning, that are, $z_1$=218.4033, $z_2$= –218.4033, $z_3$=110.9054$i$, and $z_4$= –110.9054$i$ respectively. It is clear to see that $z_3$ and $z_4$ are brush off. The $z_2$ is only preferred solution in terms of the reference configuration of Fig. 1.

Then, in order to verify further other configurations, take a trigonometric sine curve as each actuated joint input trajectory, which are shown in Fig. 6 (*a*), i.e. $d_1 = -260 - 60\times sin(\pi t)$, $d_2 = -260 - 60\times sin(3\pi t/2)$, $d_3 = -260 + 60\times sin(\pi t)$, and $d_4 = -260 + 60\times sin(3\pi t/2)$ respectively. Based on above analysis and the forward kinematic solutions in previous section, we obtain the path of the gripper on the moving platform shown in Fig. 6 (*b*).

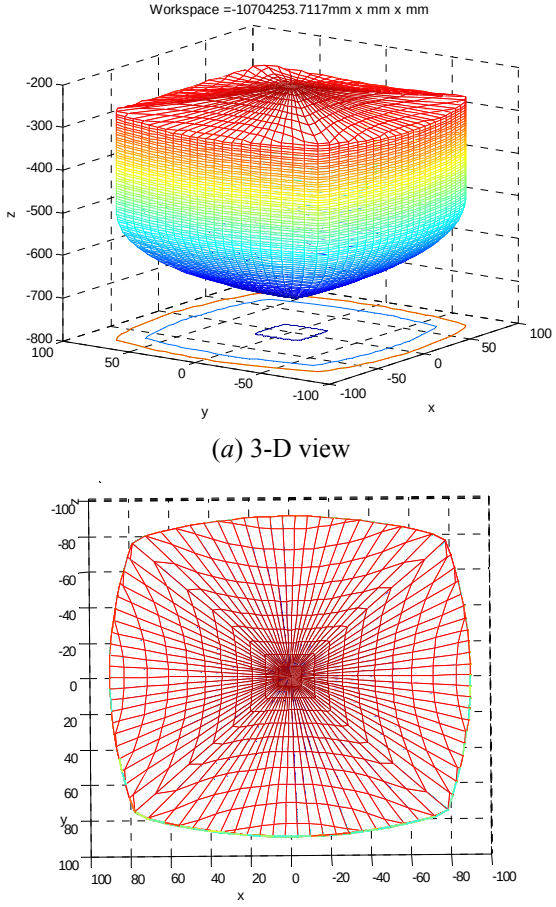


(*a*) 3-D view

(*b*) Top-view

Fig. 7. The workspace of a RASTPR

## 5.3 Workspace

The workspace of a PR is one of the most important aspects to reflect its performance, and it is necessary to analyze the shape and volume of the workspace for enhancing applications of PRs. The reachable workspace boundary and volume of a RASTPR are determined by a numerical method, in terms of its inverse kinematic solutions in previous section.

Equation (20)~(23) represent the workspace of the $i$-th ($i$=1,2,3,4) limb, which is a set of cylinders with the radii of ($l_3$+2$l_2$). The robot workspace can be

derived geometrically by the intersection of the four limbs' workspace. Assume that $d_1 = 0$, $d_2 = 0$, $d_3 = 0$, and $d_4 = 0$ is the initial configuration of a RASTPR. To determine the boundary of the workspace, we adopt a simply numerical search method, that is, so-called the layered left-right search algorithm (LLRSA). The algorithm central idea that is, the entire workspace is divided into many layers along $z$ axis, each layer is divided into some sectors, and the sectors radius are determined via inverse kinematics and some constraint of joints, so the sectors boundary and volume are determined. The workspace volume is approximately calculated as the sum of all sectors volume.

Taking the mentioned geometrical parameters above, the workspace and volume of the RASTPR are shown in Fig. 7. It is obvious that there is regular shape, which is a cubical approximately. Additionally, it has the workspace advantage along $z$ axis, if the actuation stroke is long enough.

# 6 Conclusion

In this paper, a novel redundant actuated PR with four identical $PRP_AR$ topology limbs is proposed. After a short description of the novel architecture, its kinematic modeling is built through the D-H parametric notions and the coordinate transformation technique, which verify that this novel PR has pure spatial translational motion. Follow these analysis, the inverse and forward kinematic problem are solved with analytical closed-form. Finally, a case study is analyzed by numerical method, including the determination of workspace, simulation of the inverse and forward kinematic solutions. We can conclude that:

(1) The well known D-H parametric notions and the coordinate transformation technique can be applied in the analysis of motion properties of a PR.

(2) The proposed RASTPR has only one inverse kinematic solution with analytical closed-form for each actuated joint. Also, its forward kinematic solution has only one feasible solution by the assembly manner. These advantages are key issues for path and trajectory planning, and real time control.

(3) The workspace of novel RASTPR has regular shape, which is a cubical approximately, and it has the workspace advantage along $z$ axis,

As for the future works of this novel RASTPR, we propose the dynamic modeling and control issues for polishing application.

**Acknowledgment**

The authors appreciate the fund support from National Natural Science Foundation of China (No. 50575208), and Zhejiang Province Natural Science Foundation (No. M503099).

*References:*

[1] Merlet, J. P., Redundant Parallel Manipulators, *Laboratory Robotics and Automation*, Vol. 8, No. 1, 1996, pp. 17–24.

[2] Kim, S., Operational Quality Analysis of Parallel Manipulators with Actuation Redundancy, *Proc. of the IEEE Int. Conf. on Robotics and Automation*, Albuquerque, New Mexico, 1997, pp. 2651-2656.

[3] Kock, S., and Schumacher, W., A Parallel *x-y* Manipulator with Actuation Redundancy for High-Speed and Active-Stiffness Applications, *Proc. of the IEEE Int. Conf. on Robotics and Automation*, Leuven, Belgium, 1998, pp. 2295–2300.

[4] Liu, G. F., et al., Analysis and Control of Redundant Parallel Manipulators, *Proc. of the IEEE Int. Conf. on Robotics and Automation*, Seoul, Korea, 2001, pp. 3748–3754.

[5] Liao H., et al., Singularity Analysis of Redundant Parallel Manipulators, *IEEE Int. Conf. on Systems, Man and Cybernetics*, 2004, pp. 4212-4220.

[6] Sadjadian, H., and Taghirad, H. D., Kinematic analysis of the hydraulic shoulder: a 3-DOF redundant parallel manipulator, *IEEE Int. Conf. on Mechatronics & Automation,* Niagara, 2005, pp. 1442-1446.

[7] Kim, J., et al. Designed and Analysis of a Redundantly Actuated Parallel Mechanism for Rapid Machining, *IEEE Trans. Robotics and Automation*, Vol.17, No.4, 2001, pp. 423-434.

[8] Siciliano, B., The Tricept Robot: Inverse Kinematics, Manipulability Analysis and Closed-loop Direct Kinematics Algorithm. *Robotica*, Vol. 17, 1999, pp. 437- 445.

[9] Joshi, S. A., and Tsai, L. W., The kinematics of a class of 3-DOF 4-legged parallel manipulators, *ASME J. Mech. Design,* Vol. 125, No. 1, 2003, pp. 52–60.

[10] Joshi, S. A., and Tsai, L. W., A comparison study of two 3-DOF parallel manipulators: one with three and the other with four supporting legs, *IEEE Trans. on Robotics & Automation*, Vol. 19, No. 2, 2003, pp. 200-209.